Synthesis and crystal structure refinement by the Rietveld method of antimony-bearing titanite $Ca(Ti_{0.6}Al_{0.2}Sb_{0.2})OSiO_4$

Fernando Colombo[a)]
Cátedra de Geología General, Facultad de Ciencias Exactas, Físicas y Naturales, Universidad Nacional de Córdoba, Vélez Sarsfield 1611, 5000 Córdoba, Argentina

Elisa V. Pannunzio Miner
INFIQC-CONICET, Facultad de Ciencias Químicas, Universidad Nacional de Córdoba, Ciudad Universitaria s/n, 5000 Córdoba, Argentina

(Received 19 August 2008; accepted 20 June 2009)

A synthetic analogue, $Ca(Ti_{0.6}Al_{0.2}Sb_{0.2})OSiO_4$, of antimony-bearing titanite of a composition similar to that found at St. Marcel-Praborna (Italy) was synthesized using ceramic methods and the crystal structure was refined using the Rietveld method. Unit-cell dimensions (in Å) are $a=7.0184(1)$, $b=8.7097(2)$, $c=6.5586(1)$, and $\beta=113.700(1)°$. The substitution of 40% Ti by (Al+Sb) in octahedra causes a loss of long-range coherency of the off-centered Ti atoms. The space group of Sb-bearing titanite is $A2/a$, like other cases of M^{3+}-M^{5+}-doped titanites. This study confirms that titanite with up to 0.2 Sb atom per f.u. can exist and that the substitution scheme is $2Ti^{4+} \leftrightarrow Al^{3+}+Sb^{5+}$. © *2009 International Centre for Diffraction Data.* [DOI: 10.1154/1.3194249]

Key words: doped titanite, antimony, Rietveld refinement

I. INTRODUCTION

Titanite is a widespread accessory mineral in igneous and metamorphic rocks, where it is an important host of rare-earth elements, Nb, Ta, and U, among others, and so has a large influence on geochemical modeling. It has also been used for isotopic dating since it has a closure temperature of approximately 600 °C. The ability to incorporate radioactive materials such as ^{92}Nb makes titanite a potential material for immobilization of such isotopes. It has also been studied by material scientists due to its structural similarity with $KTiPO_5$, a compound with optical applications widely used in lasers.

In certain exotic geochemical environments, elements other than those mentioned above can enter the titanite structure. Perseil and Smith (1995) reported antimony-bearing titanite from Mn-rich quartzite located at Saint Marcel-Praborna, in the Aosta Valley, Italy. Microprobe analyses show that this titanite can have up to 12.59% Sb_2O_5, equivalent to 0.165 Sb^{5+} atom per f.u. (apfu). Unfortunately, from the point of view of structure studies, the material is highly inhomogeneous, with Sb-rich zones mostly concentrated along grain borders and microfractures or in inclusions and pores. The very small size of the Sb-rich domains is a further complication for the study of this phase by single-crystal methods. The incorporation of other pentavalent cations such as Ta and Nb has been studied in detail but there are as yet no data on Sb-bearing titanite. Therefore we synthesized titanite with a composition of $Ca(Ti_{0.6}Al^{+3}{}_{0.2}Sb^{5+}{}_{0.2})OSiO_4$, a composition with slightly more Sb than the Sb-richest sample reported by Perseil and Smith (1995) in order to investigate the influence of Sb-Al incorporation in the titanite structure.

a)Author to whom correspondence should be addressed. Electronic mail: fcolombo@com.uncor.edu

II. THE TITANITE STRUCTURE: AN OVERVIEW

The structural formula of titanite can be represented as $^{[7]}X^{[6]}Y\,^{[4]}TO_5$, where numbers in square brackets indicate the coordination number of the site. In ideal titanite, $^{[7]}X$ is occupied by Ca, $^{[6]}Y$ by Ti, and $^{[4]}T$ by Si, but extensive substitutions in both natural and synthetic titanite have been described (e.g., Clark, 1974; Paul *et al.*, 1981; Hollabaugh and Foit, 1984; Groat *et al.*, 1985; Bernau and Franz, 1987; Oberti *et al.*, 1991; Enami *et al.*, 1993; Russell *et al.*, 1994; Černý *et al.*, 1995; Perseil and Smith, 1995; Della Ventura *et al.*, 1999; Chakhmouradian, 2004; Liferovich and Mitchell, 2006a). The main schemes that incorporate pentavalent cations in the titanite structure are $2Ti^{4+} \leftrightarrow M^{3+}+M^{5+}$ (single site, where M is usually Al or Fe for 3+ cations and Ta or Nb for 5+ cations) and $^{[7]}Ca^{2+}+{}^{[6]}Ti^{4+} \leftrightarrow {}^{[7]}Na^{+}+{}^{[6]}M^{5+}$. A number of substitutions involving ions with other valencies are also possible, including $Ti^{4+}+O^{2-} \leftrightarrow M^{3+}+(F,OH)^{-}$, $Si^{4+}+O^{2-} \leftrightarrow Al^{3+}+(F,OH)^{-}$, and substitutions for homovalent elements in a single site (among others, Zr^{4+}, Sn^{4+} for Ti^{4+} or Ba^{2+}, Sr^{2+}, or Mn^{2+} for Ca^{2+}). Of particular interest is the incorporation of radioactive elements (mainly U and Th, which substitute for Ca), allowing the use of titanite for geochronological work; these elements may also cause important structural damage, leading sometimes to metamictization (Hawthorne *et al.*, 1991; Salje *et al.*, 2000; Zhang *et al.*, 2000).

The titanite structure and its displacive phase transitions have been reviewed by many workers (e.g., Spears and Gibbs, 1976; Taylor and Brown, 1976; Bismayer *et al.* 1992; Kek *et al.*, 1997; Zhang *et al.* 1997; Ellemann-Olesen and Malcherek, 2005; Liferovich and Mitchell, 2006a, 2006c), so just a brief review will be made here.

The titanite structure has kinked chains of corner-sharing YO_6 octahedra along [100], cross-linked by SiO_4 tetrahedra. Ca occupies interstitial irregular sites of sevenfold coordination. The space group of pure $CaTiOSiO_4$ is $P2_1/a$. Ti atoms are displaced from the geometric center of the octahedra,

along $+a$ in a single chain and along $-a$ in the chain related to the first one by the center of symmetry, resulting in antiferroelectric interactions. The off centering is caused by a second-order Jahn-Teller effect due to the d^0 configuration of Ti^{4+} and its sixfold coordination (Kunz and Brown, 1995).

Titanite can undergo displacive phase transitions from space group $P2_1/a$ to $A2/a$, caused by variations in pressure, temperature, or incorporation of additional elements. In this case Ti-O electric dipoles are either nonexistent or lack long-range order, thus showing paraelectric behaviour. Since the nonstandard $A2/a$ space group has been used by most of the authors (instead of $C2/c$), we will continue to use it for ease of comparison. A structurally related compound $Ca(Ti_{1-x}Zr_x)OGeO_4$ shows a further phase transition from $A2/a$ to $A\bar{1}$ at room temperature for $x>0.68$ (Ellemann-Olesen and Malcherek, 2005). There is a phase transition from $P2_1/a$ to $A2/a$ at room temperature and elevated pressure [between 35 and 36 kbars, according to Knoche *et al.* (1998) and Angel *et al.* (1999) by the actual centering of Ti atoms in octahedra to avoid an increase in overbonding (Kunz *et al.*, 1996)]. At a pressure of 105 kbars another phase transition occurs, with a change to space group $P\bar{1}$ (Rath *et al.*, 2001). On the other hand, a nonquenchable $P2_1/a \rightarrow A2/a$ transition can result not from centering of Ti atoms in their coordination polyhedra but from loss of long-range coherency of the Ti-O displacement vectors due to a temperature increase above 496 K at ambient pressure (Bismayer *et al.*, 1992; Zhang *et al.*, 1995). Zhang *et al.* (1997) suggested that at approximately 825 K a displacement of Ti towards the center of the octahedral site may occur, leading to a true $A2/a$ symmetry.

The transition to the $A2/a$ space group caused by the entry of other ions in the titanite structure (either exclusively at the Ti site or combinations of several sites) is also probably caused by loss of long-range coherency, relieving of underbonding of anions located at the O(1) position and formation of antiphase boundaries (Higgins and Ribbe, 1976; Hughes *et al.*, 1997; Liferovich and Mitchell, 2005). Therefore, this is a macroscopically disordered form, with $P2_1/a$ domains at unit-cell scale but overall $A2/a$ symmetry.

III. EXPERIMENTAL

A. Synthesis and chemical composition of the title compound

Al-Sb-bearing titanite was synthesized by solid-state reaction of a mixture of reagent-grade powders of $CaCO_3$, TiO_2, SiO_2, Sb_2O_3, and $Al(NO_3)_3 \cdot 9H_2O$ in stoichiometric proportions to give $Ca(Ti_{0.6}Sb^{5+}_{0.2}Al^{3+}_{0.2})OSiO_4$. An oxide with an Sb_2O_3 stoichiometry (where Sb has a 3+ oxidation state) was chosen over Sb_2O_5 because of the low melting point of this latter compound. Heating in air during the first part of the synthesis process resulted in oxidation of Sb along with the formation of binary Sb-bearing oxides that do not melt at the temperatures selected for the synthesis. Reagents were mixed, ground with a pestle in an agate mortar under acetone and pelletized at a pressure of 2 ton cm^{-2}. Two successive treatments with grinding in between were made: the first one at 800 °C for 30 min and a second one at 1200 °C for 12 h. Heating and cooling rates were 3 °C/min.

Impurity phases detected by X-ray diffraction were wollastonite-4*A* and $Ca_2Sb_2O_7$. Refined weight percentages were 3.7(2) and 0.60(6), respectively. A second cycle at 1200 °C for 12 h showed no change in the relative proportions of the three synthesized phases.

Antimony-bearing titanite was analyzed using a JEOL JXA 8900-M microprobe (wavelength dispersive mode) at the Centro de Microscopía Luis Brú (Universidad Complutense de Madrid). Analytical conditions were beam diameter of 1 μm, acceleration voltage of 20 kV, beam current of 50 nA, with counting times of 20 s (peak) and 10 s (at each side of the peak). The following standards were used: kaersutite (Ca,Ti), albite (Si), SbGa (Sb), and sillimanite (Al). The compositions of synthetic titanite (in wt % oxide) are SiO_2 (28.10), TiO_2 (23.79), Al_2O_3 (5.09), Sb_2O_5 (14.64), and CaO (27.51), a total of 99.13.

B. Data collection and Rietveld refinement

The X-ray diffraction powder pattern was taken at ambient pressure and 22 °C between 14° and 140° 2θ with a PANalytical X´Pert Pro diffractometer housed at the INFICQ-Facultad de Ciencias Químicas, with Bragg-Brentano geometry and a fixed divergence slit. The diagram was measured using Cu $K\alpha$ radiation (40 mA, 40 kV) and a diffracted-beam graphite monochromator. Sample was smeared onto a zero-background single-crystal Si sample holder. Observed and calculated powder diffraction data for the Sb-Al-bearing titanite at room temperature are given in Table I.

Peak positions were obtained using the X´Pert HighScore™ v.2.1.2 software using the minimum second derivative method, and interplanar distances were calculated using Cu $K\alpha_1$ ($\lambda = 1.5406$ Å). Integrated intensities were used after Cu $K\alpha_2$ stripping [performed using the Rachinger method (Rachinger, 1948)]. *hkl* values were assigned by comparison with compounds with similar structures, such as $CaTiOSiO_4$ doped with Nb, Ta, and Al (space group $A2/a$). In cases where the assignment was not straightforward the *hkl* list generated by FULLPROF (see below) was used. Figures of merit are $M_{20}=129$ (as defined by de Wolff, 1968) and $F_{30}=97$ (0.0060; 51) (as defined by Smith and Snyder, 1979).

The experimental and calculated patterns were treated in the same way in order to obtain the values reported in Table I.

Rietveld refinements were made with the FULLPROF software (Roisnel and Rodríguez-Carvajal, 2007), version September 2007, using the atomic coordinates and atomic displacement parameters of Nb-bearing titanite from Liferovich and Mitchell (2006a) as starting values. The refinement was performed using two wavelengths (Cu $K\alpha_1$ and Cu $K\alpha_2$) with a 2:1 intensity ratio. Cationic proportions at the Ca and Ti sites were set according to the target stoichiometry and refined at the latest cycles of the refinement process, with total occupancy of each site constrained to unity (and Sb = Al, in apfu). A pseudo-Voigt function was used for peak shape modeling. Refined parameters included scale, background (a polynomial function with seven parameters), unit-cell dimensions, zero shift, W, U, V, η, X, asymmetry, atomic coordinates, site occupancies, and isotropic atomic displacement parameters. Ionized scattering factors were used for all atoms. Structures used for modeling impurity phases

TABLE I. Observed and calculated powder diffraction data for $Ca(Ti_{0.6}Al_{0.2}Sb_{0.2})OSiO_4$ at room temperature.

Observed						Calculated			
2θ (deg)	d (Å)	I (%)	h	k	l	2θ (deg)	d (Å)	I (%)	$\theta 2\Delta$
17.935	4.9417	34.7	0	1	1	17.943	4.9395	32.7	−0.008
			−1	1	1	18.67	4.7488	0.3	
20.384	4.3533	4.1	0	2	0	20.39	4.352	3.9	−0.006
			1	2	0	24.683	3.604	0.2	
26.114	3.4096	0.9	1	1	1	26.112	3.4099	0.9	0.002
27.637	3.2251	100	−2	1	1	27.638	3.225	100	−0.001
29.733	3.0023	80.7	0	0	2	29.736	3.0021	72.4	−0.003
31.539	2.8344	3.3	−2	0	2	31.542	2.8341	3.5	−0.003
34.285	2.6134	73.9	0	3	1	34.284	2.6135	62.6	0.001
34.674	2.585	42.9	−2	2	0	34.671	2.5852	43.1	0.003
			0	2	2	36.316	2.4718	0.1	
37.844	2.3754	5.6	−2	2	2	37.842	2.3756	4.9	0.002
38.092	2.3605	6	2	1	1	38.092	2.3605	5.5	0.000
39.391	2.2856	15.6	1	3	1	39.395	2.2854	14.8	−0.004
39.925	2.2563	8	−3	1	1	39.92	2.2565	8.9	0.005
40.483	2.2265	1.7	−2	3	1	40.469	2.2272	1.5	0.014
41.436	2.1774	3.2	0	4	0	41.441	2.1772	3.3	−0.005
42.819	2.1102	9	−1	1	3	42.812	2.1106	8.6	0.007
43.319	2.087	4.3	1	2	2	43.316	2.0872	3.6	0.003
43.832	2.0638	22.7	1	4	0	43.826	2.0641	21.8	0.006
45.930	1.9743	2.9	−3	2	2	45.929	1.9743	1.7	0.001
46.513	1.9509	9.6	0	1	3	46.508	1.9511	7.9	0.005
			3	2	0	47.248	1.9222	0.3	
			2	3	1	48.549	1.8737	0.3	
49.121	1.8532	1.8	2	0	2	49.109	1.8537	1.3	0.012
50.591	1.8028	9	−2	4	0	50.595	1.8027	9.1	−0.004
51.817	1.763	2.9	0	4	2	51.81	1.7632	2.5	0.007
52.681	1.7361	8.5	−4	0	2	52.668	1.7365	10.6	0.013
52.980	1.727	10.4	−2	4	2	52.982	1.7269	12.3	−0.002
53.701	1.7055	18	2	2	2	53.695	1.7056	16.1	0.006
54.826	1.6731	1	0	5	1	54.827	1.6731	0.9	−0.001
55.110	1.6652	1	−1	5	1	55.106	1.6653	1.1	0.004
55.736	1.6479	24.3	0	3	3	55.728	1.6481	19.2	0.008
			−4	2	2	57.05	1.6131	0.9	
57.299	1.6066	3.5	4	0	0	57.297	1.6067	3.5	0.002
58.366	1.5798	0.6	−4	1	3	58.323	1.5809	0.4	0.043
59.303	1.557	9.8	−2	5	1	59.299	1.5571	9.8	0.004
60.423	1.5308	6.6	−3	4	0	60.408	1.5312	6.5	0.015
			4	2	0	61.459	1.5075	1	
61.741	1.5013	5.3	0	0	4	61.732	1.5015	4.1	0.009
62.276	1.4897	8.9	−4	3	1	62.258	1.49	11.9	0.018
64.107	1.4514	2.3	0	6	0	64.093	1.4517	1.8	0.014
64.860	1.4364	4.4	2	1	3	64.847	1.4367	3.5	0.013
65.696	1.4201	7.9	2	5	1	65.682	1.4204	7	0.014
65.854	1.4171	6.9	−4	0	4	65.843	1.4173	8.3	0.011
66.425	1.4063	4.6	−4	3	3	66.422	1.4064	5.7	0.003
69.067	1.3588	0.4	−4	4	2	69.134	1.3577	0.5	−0.067
69.748	1.3472	6	−2	5	3	69.743	1.3473	6	0.005
71.000	1.3265	0.5	−1	6	2	70.972	1.3269	0.5	0.028
72.221	1.307	7.4	0	6	2	72.21	1.3072	6	0.011
72.914	1.2963	1.5	−2	1	5	72.9	1.2965	1.3	0.014
74.474	1.273	4	4	3	1	74.469	1.2731	4.6	0.005
76.610	1.2427	0.3	−5	3	1	76.607	1.2428	0.3	0.003
77.834	1.2262	2.9	4	0	2	77.819	1.2264	2.5	0.015
78.690	21.2144	0.6	−3	6	2	78.68	1.2151	0.8	0.010
80.836	1.1881	0.7	−4	4	4	80.846	1.188	0.5	−0.010

TABLE II. Results of the Rietveld refinement of $Ca(Ti_{0.6}Al_{0.2}Sb_{0.2})OSiO_4$.

Space group
$A2/a$ (No. 15). $Z=4$, $a=7.0184(1)$ Å; $b=8.7097(2)$ Å; $c=6.5586(1)$ Å; $\beta=113.700(1)°$, $V=367.10(1)$ Å^3

Experimental data
Temperature of 295 K; angular range of $14° \leq 2\theta \leq 140°$; step scan increment ($2\theta$) 0.02°, time per step of 4 s.

Refinement and profile parameters
Three phases: $Ca(Ti_{0.6}Al_{0.2}Sb_{0.2})OSiO_4$, $CaSiO_3$ (space group $C\bar{1}$), and $Ca_2Sb_2O_7$.
Zero point: 0.0159(5)°; number of refined parameters: 38.
Pseudo-Voigt function, PV= $\eta L+(1-\eta)G$; $\eta=0.78(1)$; $X=-0.000\,49(9)$
Half-width parameters: $U=0.0530(5)$, $V=-0.0183(5)$, $W=0.0093(2)$
Asymmetry parameters: Asym 1=0.102(3); Asym 2=0.0542(7).
Conventional Rietveld R factors (background subtracted): R_p: 14.2; R_{wp}: 16.0, R_{exp}: 11.66; χ^2: 1.88; R_{Bragg}: 4.32, and R_f: 3.77.
SCOR=1.8220 (as defined by Bérar and Lelann, 1991)
DW stat: 1.2355 DW-exp: 1.9339

Atom	Site	x	Y	z	Occupancy	U (Å^2)
Ca^{2+}	4*e*	1/2	0.1680(1)	0	1	1.53(2)
$Ti^{4+}/Sb^{5+}/Al^{3+}$	4*b*	1/2	0	1/2	0.604/0.198/0.198	0.895(9)
Si^{4+}	4*e*	3/4	0.1826(2)	0	1	0.92(2)
$O1^{-2}$	4*e*	3/4	0.0707(3)	1/2	1	1.35(3)
$O2^{-2}$	8*f*	0.9040(3)	0.0661(2)	0.1817(3)	1	1.69(2)
$O3^{-2}$	8*f*	0.3782(4)	0.2142(2)	0.3970(3)	1	1.46(2)

wollastonite-4*A* and $Ca_2Sb_2O_7$ were those of Yamanaka and Mori (1981) and Bystroem (1945), respectively. Only scale factors were refined for these two impurity phases.

More experimental details, profile parameters, agreement indices, final atomic coordinates, and equivalent isotropic atomic displacement parameters appear in Table II. The ATOMS V6.3.1 program (Dowty, 2006) was used for structure drawing and polyhedron volume calculations. Figure 1 shows the low-angle section (14° to 80° 2θ) of the observed and the Rietveld-refined diffraction patterns for $Ca(Ti_{0.6}Al_{0.2}Sb_{0.2})OSiO_4$.

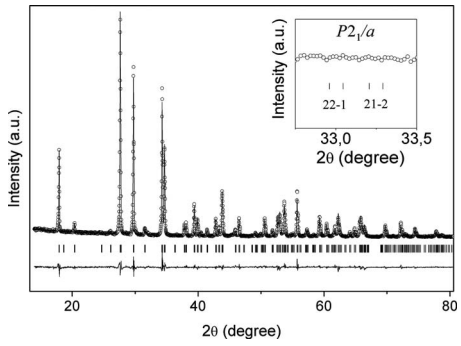

Figure 1. Experimental (circles), calculated (solid line), and difference profiles of the XRD pattern of $Ca(Ti_{0.6}Al_{0.2}Sb_{0.2})OSiO_4$. The inset displays the region between 32.75° and 33.50° (2θ), showing no features where the reflections $22\bar{1}$ and $21\bar{2}$ (diagnostic of space group $P2_1/a$) should appear. Note that although just the low-angle section of the diffraction pattern is shown here, the whole data set (14° to 140° 2θ) was used for the refinement.

IV. STRUCTURE OF Sb-Al BEARING TITANITE: RESULTS AND DISCUSSION

In the following paragraphs we describe the structure of $Ca(Ti_{0.6}Al_{0.2}Sb_{0.2})OSiO_4$ and compare it with the structures of pure $CaTiOSiO_4$ and $Ca(Ti_{0.6}Al_{0.2}X_{0.2})OSiO_4$ ($X=Nb^{5+}$, Ta^{5+}) when pertinent. We will refer to these last two phases as Nb titanite and Ta titanite. A parameter that has been used to compare titanite structures is the distortion index (Oberti *et al.*, 1991; Liferovich and Mitchell, 2006a, 2006c). The distortion index (defined by Shannon 1976) is a useful parameter to quantify distortions in polyhedra when no appreciable variation in bond angles occurs. It is defined as $\Delta_n = (1/n)\ 10^3\Sigma[(r_i-\bar{r})/\bar{r}]^2$, where r_i is an individual bond length and $\bar{r}$ is the average bond length in the polyhedron. The bond-angle variance index (proposed by Robinson *et al.*, 1971) is defined as $\delta_n=[1/(n-1)]*[\Sigma(\theta_i-\theta_n)^2]$, where θ_I represents the angle value calculated from the structure refinement and θ is the ideal angle for the polyhedron (90° in an octahedron or 109.47° in a tetrahedron).

It has long been known (e.g., Higgins and Ribbe, 1976; Hollabaugh and Foit, 1984) that unit-cell dimensions in titanite-structured compounds are related to the size of cations occupying the Y site. The a, b, and c dimensions of Sb titanite are smaller than those of pure $CaTiOSiO_4$, Nb and Ta titanites (Table III), whereas no correlation was noted between β and the average size of the cations in the Y site (using the crystal radii of Shannon, 1976). These correlations are even more clearly defined when other cations in the Y site are considered, such as Zr (Chakhmouradian, 2004) and Sn [in the isostructural mineral malayaite (Zhang *et al.*, 1999)].

TABLE III. Unit-cell parameters of synthetic $CaTiOSiO_4$ (space group $P2_1/a$) and $Ca(Ti_{0.6}Al_{0.2}X_{0.2})OSiO_4$ (X=Sb^{5+}, Nb^{5+}, Ta^{5+}) (space group $A2/a$) at ambient conditions.

	Sb^{+5}	Nb^{+5}	Ta^{+5}	$CaTiOSiO_4$
a (Å)	7.0184(1)	7.0594(1)	7.0610(1)	7.0697(3)
b (Å)	8.7097(2)	8.7188(1)	8.7162(2)	8.7223(4)
c (Å)	6.5586(1)	6.5651(1)	6.5697(1)	6.5654(4)
β (deg)	113.700(1)	113.747(1)	113.742(1)	113.853(4)
V (Å^3)	367.10(1)	369.86(1)	370.11(1)	370.27(1)
Reference	This work	Liferovich and Mitchell (2006a)	Liferovich and Mitchell (2006c)	Kek *et al.* (1997)

Pure $CaTiOSiO_4$ adopts space group $P2_1/a$ at room temperature; the entry of dopants (at least 10% molar) produces a change to space group $A2/a$. Therefore, it was expected that Sb-Al-bearing titanite would also have this space group. Extinction rules in $A2/a$ forbid reflections with $k+l=2n+1$, while they are allowed by space group $P2_1/a$. Due to severe overlap of diagnostic reflections, the most reliable reflections to differentiate between the two mentioned space groups are $22\bar{1}$ and $21\bar{2}$ (Kunz *et al.* 1996). A scan between 32° and 33.9° (2θ) with a counting time of 10 s per step shows no peaks (see the inset of Figure 1), suggesting that the correct space group for titanite with 0.2 apfu Sb^{5+} and 0.2 apfu Al^{3+} is $A2/a$. As a further check we refined the data set in space group $P2_1/a$, with agreement indices that were not as good as those obtained using the space group $A2/a$.

Even though the cause of the transition (centering of atoms in the Y site or loss of long-range electric dipole order) cannot be determined using conventional X-ray diffraction, we strongly support the second option as the most likely cause for the space group transition.

The general structural features coincide with those already known for titanite, as described in Sec. III. The atomic structure is shown in Figure 2. Bond lengths, polyhedron volumes, and some distortion parameters appear in Table IV.

No Sb or vacancies are found to present in the $^{[7]}X$ site by the Rietveld refinement. According to the distortion index, the sevenfold polyhedron of Sb-titanite is more distorted than the equivalent polyhedron of Nb or Ta titanites, and in this respect it is very similar to that of $CaTiOSiO_4$.

Refined occupancies in the $^{[6]}Y$ site are 0.604 Ti, 0.198 Al, and 0.198 Sb apfu, in good agreement with theoretical occupancies: 0.60 Ti, 0.20 Al, and 0.20 Sb apfu. No reflections with $h0l$, where h=odd, were detected that would evidence ordering of cations in the Y site (Hollabaugh and Foit, 1984). Distortion parameters Δ_6 and δ_6 are similar to those of Nb and Ta titanites and are smaller than those corresponding to $CaTiOSiO_4$, indicating that octahedra in substituted titanite are more symmetrical.

Tetrahedral Al^{3+} replacing Si^{4+} cannot be detected using conventional X-ray diffraction, so the mean $\langle T\text{-O}\rangle$ bond length is usually evaluated as an indirect indicator of Al-for-Si substitution. As reviewed by Liferovich and Mitchell (2006a, 2006c), mean $\langle$Si–O$\rangle$ distances in silicates with ordered Al-Si distribution are in the range of 1.608 to 1.624 Å. The Si-O2 and Si-O3 distances in Sb titanite are quite similar to each other; the mean $\langle$Si–O$\rangle$ bond length is 1.60(1) Å, much shorter than typical $\langle$Al-O$\rangle$ bond lengths. Therefore, we infer that no appreciable Al-for-Si substitution occurred.

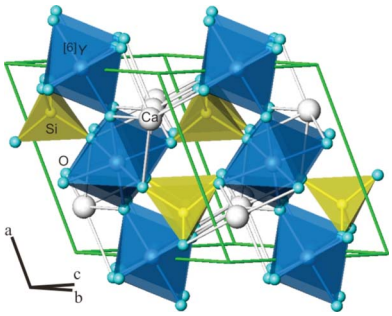

Figure 2. (Color online) View of the crystal structure of $Ca(Ti_{0.6}Al_{0.2}Sb_{0.2})OSiO_4$. The symbol $^{[6]}Y$ stands for sixfold-coordinated Ti, Sb, and Al in a 2:1:1 ratio. The small light grey spheres are O atoms.

TABLE IV. Selected bond lengths (in Å, at ambient conditions) of $CaTiOSiO_4$ (space group $P2_1/a$) and $Ca(Ti_{0.6}Al_{0.2}X_{0.2})OSiO_4$ (X=Sb^{5+}, Nb^{5+}, Ta^{5+}) (space group $A2/a$). Data source: Kek *et al.* (1997), Liferovich and Mitchell (2006a, 2006c), this work. DI=distortion index (Shannon, 1976). BAVI=bond-angle variance index (Robinson *et al.*, 1971). BVS =bond valence sum (in valence units).

	X=Sb^{5+}	X=Nb^{5+}	X=Ta^{5+}	$CaTiOSiO_4$
Ca–O1	2.275(3)	2.284(6)	2.308(7)	
Ca–O2 (2x)	2.390(2)	2.411(4)	2.409(5)	
Ca–O3 (2x)	2.420 (2)	2.465(4)	2.463(5)	
Ca–O3′ (2x)	2.627(3)	2.599(5)	2.611(6)	
Mean$\langle$Ca–O$\rangle$	2.45(2)	2.46(2)	2.47(4)	2.457(1)
V_{CaO7} (Å^3)	19.841	19.974	20.136	19.662
DI (Δ_7)	2.43	1.75	1.72	2.42
BVS (should be 2.000)	1.996(5)	1.911	1.878	1.960
Y–O1 (2x)	1.8595(9)	1.863(2)	1.856(2)	1.872
Y–O2 (2x)	2.003(2)	2.013(4)	2.008(4)	
Y–O3 (2x)	2.051(2)	2.014(4)	2.012(4)	
Mean$\langle$Y–O$\rangle$	1.97(1)	1.96(2)	1.96(2)	1.959(1)
V_{YO6} (Å^3)	10.176	10.062	9.994	9.969
DI (Δ_6)	1.70	1.31	1.37	2.20
BAVI (δ_6)	1.69	1.85	0.76	9.40
BVS (should be 4.000)	4.034	4.000	4.084	4.211
Si–O2 (2x)	1.607(2)	1.610(4)	1.606(5)	
Si–O3 (2x)	1.602(3)	1.632(6)	1.636(7)	
Mean$\langle$Si–O$\rangle$	1.61(1)	1.62(2)	1.62(2)	1.647(1)
V_{SiO4} (Å^3)	2.105	2.168	2.169	2.283
DI (Δ_4)	0.00	0.05	0.09	0.02
BAVI (δ_4)	14.85	20.67	17.79	12.66
BVS (should be 4.000)	4.22(2)	4.031	4.039	3.756

Bond lengths are quite similar to each other, leading to a Δ_4 of 0.00; tetrahedrons are less distorted than those of Nb or Ta titanite, as shown by the δ_4 value.

V. CONCLUSIONS

Antimony can enter the titanite structure at a level up to of at least 0.2 apfu according to the heterovalent exchange mechanism $2Ti^{4+} \leftrightarrow Al^{3+} + Sb^{5+}$. This confirms the proposal of Perseil and Smith (1995) and Smith and Perseil (1997). The single-site substitution affects the coherency of the off centering of the $^{[6]}Y$ atoms and results in an antiferroelectric-to-paraelectric transition. The space group of Sb-rich titanite at ambient pressure and temperature is $A2/a$, like other cases of M^{3+}-M^{5+}-doped titanites. Unit cell dimensions (a, b, and c) are smaller than those of pure $CaTiOSiO_4$ and Nb- and Ta-substituted titanites.

ACKNOWLEDGMENTS

We thank Raúl Carbonio (INFICQ-Universidad Nacional de Córdoba) for access to the laboratory facilities and diffractometer. Roger Mitchell (Lakehead University) kindly sent a copy of one of his publications. Thanks are also due to Jim Nizamoff (Omaya, Inc., USA) for reviewing the grammar and to José González del Tánago (Universidad Complutense de Madrid) for access to the electron microprobe. This study was funded by CONICET. We gratefully acknowledge the suggestions of M. Delgado (Universidad de Los Andes, Venezuela), the Editor-in-Chief of PF, and Ting Huang.

Angel, R. J., Kunz, M., Miletich, R., Woodland, A. B., Koch, R., and Xirouchakis, D. (**1999**). "High-pressure phase transition in $CaTiOSiO_4$ titanite," Phase Transitions **68**, 533–543.

Bérar, J.-F. and Lelann, P. (**1991**). "E.S.D.'s and estimated probable error obtained in Rietveld refinements with local correlations," J. Appl. Crystallogr. **24**, 1–5.

Bernau, R. and Franz, G. (**1987**). "Crystal chemistry and genesis of Nb-, V-, and Al-rich metamorphic titanite from Egypt and Greece," Can. Mineral. **25**, 695–705.

Bismayer, D., Schmahl, W., Schmidt, C., and Groat, L. A. (**1992**). "Linear birefringence and X-ray diffraction studies of the structural phase transition in titanite, $CaTiSiO_5$," Phys. Chem. Miner. **19**, 260–266.

Bystroem, A. (**1945**). "Calcium pyroantimonates and similar compounds," Ark. Kemi, Mineral. Geol.," **18**, 8.

Černý, P., Novák, M., and Chapman, R. (**1995**). "The $Al(Nb,Ta)Ti_{-2}$ substitution in titanite: The emergence of a new species?," Mineral. Petrol. **52**, 61–73.

Chakhmouradian, A. R. (**2004**). "Crystal chemistry and paragenesis of compositionally unique (Al-, Fe-, Nb-, and Zr-rich) titanite from Afrikanda, Russia," Am. Mineral. **89**, 1752–1762.

Clark, A. M. (**1974**). "A tantalum-rich variety of sphene," Miner. Mag. **39**, 605–607.

de Wolff, P. M. (**1968**). "A simplified criterion for the reliability of a powder pattern indexing," J. Appl. Crystallogr. **1**, 108–113.

Della Ventura, G., Bellatreccia, F., and Williams, C. T. (**1999**). "Zr- and *LREE*-rich titanite from Tre Croci, Vico Volcanic complex (Latium, Italy)," Miner. Mag. **63**, 123–130.

Dowty, E. (**2006**). ATOMS5.0: Shape software, Kingsport, Tennessee 37663, USA, http://shapesoftware.com/

Ellemann-Olesen, R. and Malcherek, T. (**2005**). "Temperature and composition dependence of structural phase transitions in $Ca(Ti_xZr_{1-x})OGeO_4$," Am. Mineral. **90**, 687–694.

Enami, M., Suzuki, K., Liou, J. G. and Bird, D. K. (**1993**). "$Al-Fe^{3+}$ and F-OH substitutions in titanite and constraints on their P-T dependence," Eur. J. Mineral. **5**, 219–231.

Groat, L. A., Carter, R. T., Hawthorne, F. C., and Ercit, T. S. (**1985**). "Tantalian niobian titanite from the Irgon Claim, Southeastern Manitoba," Can. Mineral. **23**, 569–571.

Hawthorne, F. C., Groat, L. A., Raudsepp, M., Ball, N. A., Kimata, M., Spike, F. D., Gaba, R., Halden, N. M., Lumpkin, G. R., Ewing, R. C., Greegor, R. B., Lytle, F. W., Ercit, T. S., Rossman, G. R., Wicks, F. J., Ramik, R. A., Sherriff, B. L., Fleet, M. E., and McCammon, C. (**1991**). "Alpha-decay damage in titanite," Am. Mineral. **76**, 370–396.

Higgins, J. B. and Ribbe, P. H. (**1976**). "The crystal chemistry and space groups of natural and synthetic titanites," Am. Mineral. **61**, 878–888.

Hollabaugh, C. L. and Foit, F. F., Jr. (**1984**). "The crystal structure of an Al-rich titanite from Grisons, Switzerland," Am. Mineral. **69**, 725–732.

Hughes, J. M., Bloodaxe, E. S., Hanchar, J. M., and Foord, E. E. (**1997**). "Incorporation of rare earth elements in titanite: Stabilization of the $A2/a$ dimorph by creation of antiphase boundaries," Am. Mineral. **82**, 512–516.

Kek, S., Aroyo, M., Bismayer, U., Schmidt, C., Eichhorn, K., and Krane, H. G. (**1997**). "The two-step phase transition of titanite, $CaTiSiO_5$: A synchrotron radiation study," Z. Kristallogr. **212**, 9–19.

Knoche, R., Angel, R. J., Seifert, F., and Fliervoet, T. F. (**1998**). "Complete substitution of Si for Ti in titanite $Ca(Ti_{1-x}Si_x)^{IV}Si^{IV}O_5$," Am. Mineral. **83**, 1168–1175.

Kunz, M. and Brown, I. D. (**1995**). "Out-of-center distortions around octahedrally coordinated d^0 transition metals," J. Solid State Chem. **115**, 395–406.

Kunz, M., Xirouchakis, D., Lindsley, D. H., and Häusermann, D. (**1996**). "High-pressure phase transition in titanite ($CaTiOSiO_4$)," Am. Mineral. **81**, 1527–1530.

Liferovich, R. P. and Mitchell, R. H. (**2005**). "Composition and paragenesis of Na-, Nb- and Zr-bearing titanite from Khibina, Russia, and crystal-structure data for synthetic analogues," Can. Mineral. **43**, 795–812.

Liferovich, R. P. and Mitchell, R. H. (**2006a**). "Solid solutions of niobium in synthetic titanite," Can. Mineral. **44**, 1089–1097.

Liferovich, R. P. and Mitchell, R. H. (**2006b**). "Crystal structure of a synthetic aluminoan tantalian titanite: A reconnaissance study," Miner. Mag. **70**, 115–121.

Liferovich, R. P. and Mitchell, R. H. (**2006c**). "Tantalum-bearing titanite: Synthesis and crystal structure data," Phys. Chem. Miner. **33**, 73–83.

Oberti, R., Smith, D. C., Rossi, G., and Caucia, F. (**1991**). "The crystal-chemistry of high-aluminium titanites," Eur. J. Mineral. **3**, 777–792.

Paul, B. J., Černý, P., Chapman, R., and Hinthorne, J. R. (**1981**). "Niobian titanite from the Huron claim pegmatite, Southeastern Manitoba," Can. Mineral. **19**, 549–552.

Perseil, E.-A. and Smith, D. C. (**1995**). "Sb-rich titanite in the manganese concentrations at St. Marcel-Praborna, Aosta Valley, Italy: Petrography and crystal-chemistry," Miner. Mag. **59**, 717–734.

Rachinger, W. A. (**1948**). "A correction for the α_1: α_2 doublet in the measurement of widths of X-ray diffraction lines," J. Sci. Instrum. **25**, 254–259.

Rath, S., Kunz, M., and Miletich, R. (**2001**). "Phase transition mechanisms in the mineral titanite $CaTiOSiO_4$ under high pressure—a X-ray single crystal study between 7 GPa and 10 GPa," American Geophysical Union, Fall Meeting (unpublished), Abstract No. P21B-0529.

Robinson, K., Gibbs, G. V., and Ribbe, P. H. (**1971**). "Quadratic elongation: A quantitative measure of distortion in coordination polyhedra," Science **172**, 567–570.

Roisnel, T. and Rodríguez-Carvajal, J. (**2007**). FULLPROF: Free access software for processing of X-ray diffraction data, http://www.cdifx.univ-rennes1.fr/winplotr/winplotr.htm

Russell, J. K., Groat, L. A., and Halleran, A. A. D. (**1994**). "LREE-rich niobian titanite from Mount Bisson, British Columbia: Chemistry and exchange mechanisms," Can. Mineral. **32**, 575–587.

Salje, E. K. H., Zhang, M., and Groat, L. A. (**2000**). "Dehydration and recrystallization of radiation-damaged titanite under thermal annealing," Phase Transitions **71**, 173–187.

Shannon, R. D. (**1976**). "Revised effective ionic radii and systematic studies of interatomic distances in halides and chalcogenides," Acta Crystallogr., Sect. A: Cryst. Phys., Diffr., Theor. Gen. Crystallogr. **32**, 751–767.

Smith, D. C. and Perseil, E.-A. (**1997**). "Sb-rich rutile in the manganese concentrations at St. Marcel-Praborna, Aosta Valley, Italy: Petrology and crystal-chemistry," Miner. Mag. **61**, 655–669.

Smith, G. S. and Snyder, R. L. (**1979**). "F_N: A criterion for rating powder diffraction patterns and evaluating the reliability of powder-pattern indexing," J. Appl. Crystallogr. **12**, 60–65.

Spears, J. A. and Gibbs, G. V. (**1976**). "The crystal structure of synthetic

titanite, $CaTiOSiO_4$, and the domain textures of natural titanites," Am. Mineral. **61**, 238–247.

Taylor, M. and Brown, G. E. (**1976**). "High-temperature structural study of the $P2_1/a \leftrightarrow A2/a$ phase transition in synthetic titanite, $CaTiSiO_5$," Am. Mineral. **61**, 435–447.

Yamanaka, T. and Mori, H. (**1981**). "The structure and polytypes of alpha-$CaSiO_3$ (pseudowollastonite)," Acta Crystallogr., Sect. B: Struct. Crystallogr. Cryst. Chem. **37**, 1010–1017.

Zhang, M., Meyer, H.-W., Groat, L. A., Bismayer, U., Salje, E., and Adiwidjaja, G. (**1999**). "An infrared spectroscopic and single-crystal X-ray study of malayaite, $CaSnTiO_5$," Phys. Chem. Miner. **26**, 546–553.

Zhang, M., Salje, E., and Bismayer, U. (**1997**). "Structural phase transition near 825 K in titanite: Evidence from infrared spectroscopic observations," Am. Mineral. **82**, 30–35.

Zhang, M., Salje, E., Bismayer, U., Unruh, H.-G., Wruck, B., and Schmidt, C. (**1995**). "Phase transition(s) in titanite CaTiSiO: An infrared spectroscopic, dielectric response and heat capacity study," Phys. Chem. Miner. **22**, 41–49.

Zhang, M., Salje, E., Malcherek, T., Bismayer, U., and Groat, L. A. (**2000**). "Dehydration of metamict titanite: An infrared spectroscopy study," Can. Mineral. **38**, 119–130.